# Adsorption of Small Gas Molecules onto Pt-Doped Single-Walled Carbon Nanotubes

**Charles See Yeung, Lei Vincent Liu, and Yan Alexander Wang***

*Department of Chemistry, University of British Columbia, Vancouver, British Columbia V6T 1Z1, Canada*

*Received: July 11, 2007; In Final Form: January 28, 2008*

The adsorption of small gaseous molecules to the metal center in Pt-doped (5,5) single-walled carbon nanotubes has been explored within density functional theory. A model system consisting of a single Pt atom residing in the middle of a carbon nanotube with capping H atoms is used for our investigation. For all gases studied, the overall process of adsorption was found to be exothermic, where the affinity strongly depended on the orientation of the molecule. By examining the density of states and molecular orbitals of these nanotube−adsorbate complexes in comparison to the bare Pt-doped nanotube, we show that the electronic structure of these materials is strongly influenced by the presence of gases. Hence, we propose an application of Pt-doped single-walled carbon nanotubes as gas sensors and hope to motivate experimental work in this field.

## 1. Introduction

Single-walled carbon nanotubes (SWCNTs) were discovered by Iijima in 1993[1] and has since then inspired substantial research in the field of nanotechnology. These macromolecules have been the focus of many recent studies, finding applicability in molecular electronics,[2−8] nanomechanics,[9−13] optics,[14−18] and sensors.[5,19−25] This class of carbon nanotubes is typically metallic or semiconducting in nature, depending on the geometric structure and chirality of the tube.[26] However, it has been shown that the electronic properties of these materials can be altered through doping[27] or functionalization.[3,28−36] Recently, our group has proposed a transformation whereby one of the carbon atoms in the sidewall is replaced with a transition metal.[37,38] This newly incorporated metal atom serves as a locus for reactivity and displays characteristics of classical organometallic complexes. In particular, our calculations have suggested that stable nanotube-coordinated platinum complexes can form by exposing Pt-doped SWCNTs to an atmosphere of CO.[38] It should be noted that unlike covalent modification, the stabilization of the Pt center by pendant CO ligands represents a novel transformation that should be easily reversible.

Much work has gone into the selective functionalization of carbon nanotubes. Sidewall modification has been achieved through a variety of mechanisms that takes advantage of the delocalized $\pi$-electron density along the backbone of the nanotube. For instance, methods such as fluorination followed by nucleophilic substitution,[39,40] addition of carbenes,[41] [1,3] dipolar cycloaddition of azomethine ylides,[42] Lewis acid-catalyzed electrophilic addition,[43] and hydroboration[36] have been employed. Direct atom incorporation into the backbone, however, remains a challenge. B- and N-doped SWCNTs have been prepared via chemical vapor deposition[44] and laser ablation[45] but with minimal control of doping position and concentration of heteroatoms embedded in the sidewall of the nanotube. Our group proposed a controlled method of N-doping via the insertion of a single N atom into a SWCNT by reaction of NO with the 5-1DB defect of single-walled carbon nanotubes.[27] The synthesis of transition metal-doped SWCNTs, however, continues to be elusive.[37,38]

Interestingly, the closely related transition metal-doped fullerenes have been prepared.[46−50] For example, cage substitution can be accomplished by evaporation of elemental Fe, Co, Ni, Rh or Ir into fullerene vapor.[46] Fullerenes that are externally doped with Pt, Ni, and Sm can also undergo a transformation whereby the metal is inserted into the structure of carbon atoms itself via laser ablation.[48] Not surprisingly, density functional theory (DFT) studies on metallofullerenes[48−50] show good level of agreement with experiment, verifying that the energy gap between the highest occupied molecular orbital (HOMO) and the lowest unoccupied molecular orbital (LUMO) decreases upon the introduction of a transition metal into pure $C_{60}$, resulting in a higher conductivity.[50]

Preliminary work from our own group[37,38] suggests a similar effect of transition metals in SWCNTs. Qualitatively, this should take place since the presence of additional metal d orbitals and their interaction with the delocalized $\pi$ electrons of the backbone of the nanotube should increase the net conductivity. In essence, the isolated metal centers are simple impurities along an otherwise all-carbon backbone. While metal-doped carbon nanotubes have not been prepared, our work here is of particular interest because the adsorption of small molecules onto these macromolecules represents an initial study of a transformation that is easily reversible in nature. If indeed the selective incorporation of metal atoms is possible, transition metal-doped SWCNTs could potentially find application as gas sensors.

The employment of nanotubes as sensors for gas molecules has been the interest of many research groups.[51−54] In particular, these nanomaterials have been shown to exhibit high sensitivities, being able to detect the presence of gases at concentrations below the order of parts per million (ppm).[54−56] The essential mechanism of operation is one where the conductivity of the SWCNT changes as a result of interaction with small molecules through a charge transfer.[51,54] While pure carbon nanotubes can detect species such as $NO_2$, $NH_3$, and $O_2$, the unfortunate drawback is that analytes that do not interact strongly with the carbon atoms on the surface of the nanotube do not trigger a response; molecules as simple as CO, $H_2O$, and $H_2$ escape detection.[51,53] Several methods have been proposed to broaden the scope of gas sensing, including the dispersion of Pd nanoparticles onto the surface of SWCNTs,[57] doping with N

* Corresponding author. E-mail: yawang@chem.ubc.ca.

10.1021/jp0753981 CCC: $40.75 
Published on Web 04/24/2008

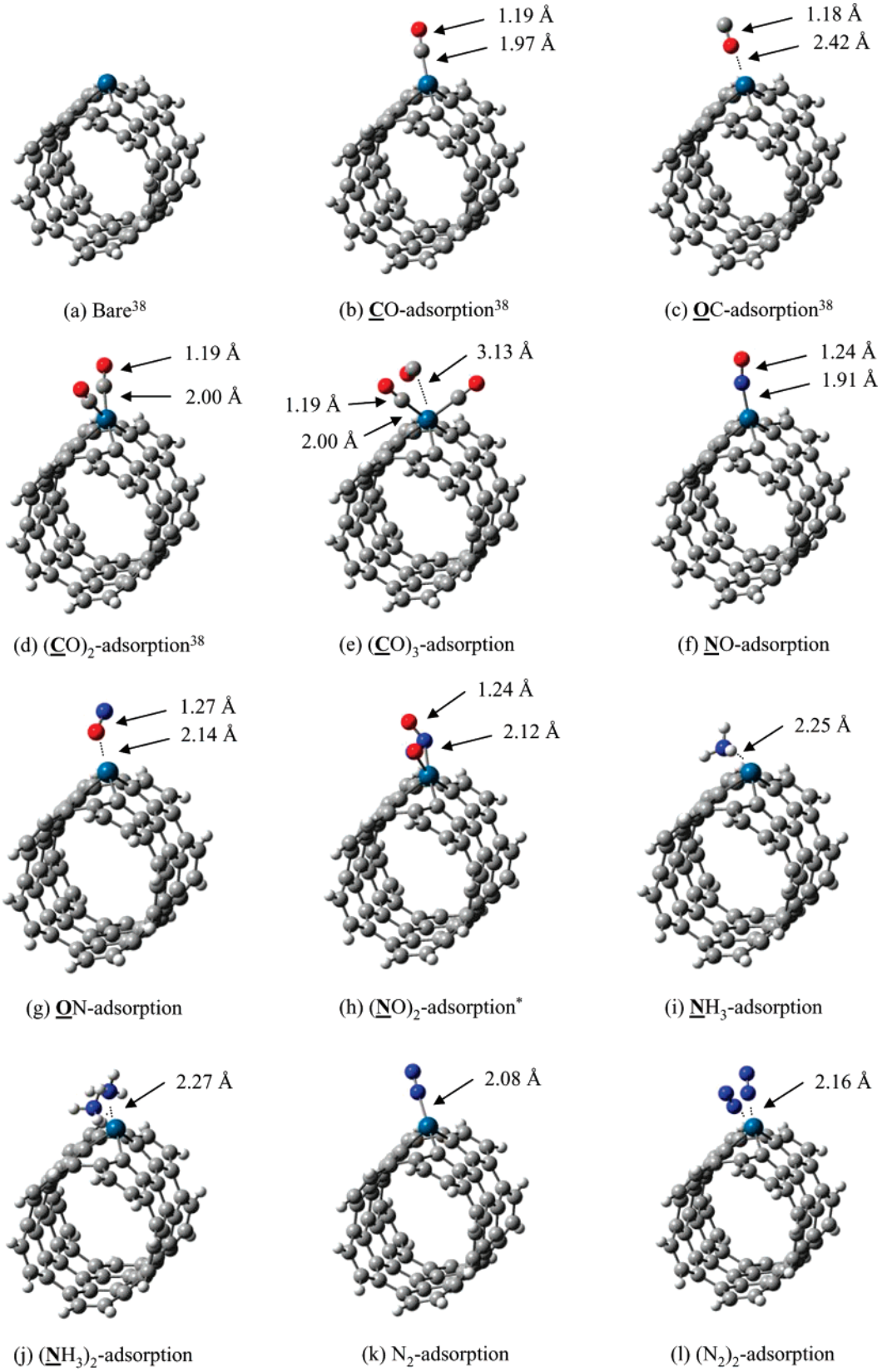


**Figure 1.** Optimized geometries of end-on adsorbed Pt-doped SWCNT fragments (Note: XY-adsorption signifies a molecule of XY has adsorbed onto the nanotube via the X atom). *See Figure 4 for an alternate perspective of this geometry.

and B,[51] and deforming the nanotube by applying a uniaxial stress, yielding an elliptical structure where the increased energetics of the system allow for interaction with otherwise undetectable species.[53] The use of transition metals in the backbone directly,[37,38] however, has not been considered. In fact, a transition metal-doped SWCNT should in theory be able to detect almost any small molecule since calculations have shown that the extended framework of the nanotube essentially acts as a supramolecular ligand.[38] In other words, if there is any precedence for a certain metal to form a complex with a given

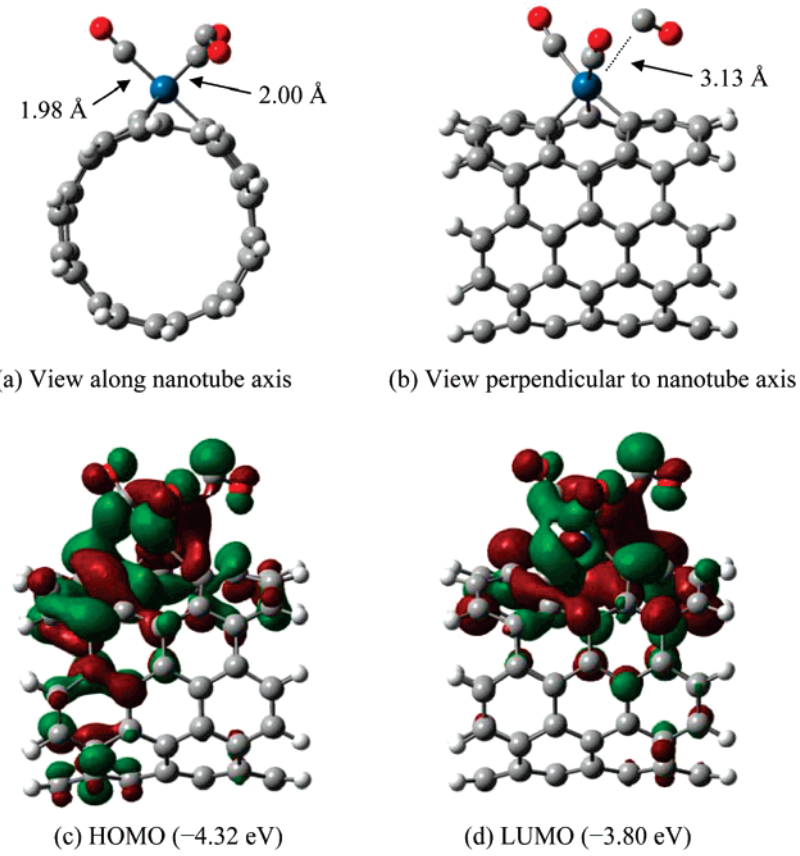


**Figure 2.** $(\underline{C}O)_3$-adsorbed Pt-doped SWCNT. The numbers in parentheses are the orbital energies in eV.

gas, the same interaction should be possible for the corresponding doped nanotube.

The metal chosen for our investigation was Pt, mainly because Pt surfaces have been shown to adsorb small gaseous molecules in a reversible and facile manner.[58−62] The inclusion of a different metal, however, will obviously affect the ability, sensitivity, and selectivity for the metal-doped nanotube to detect a certain analyte. Herein, we now disclose our findings on the effects of gas molecules including CO, NO, $NH_3$, $N_2$, $H_2$, $C_2H_4$, and $C_2H_2$ on Pt-doped SWCNTs.

## 2. Theoretical Calculations

A seventy-atom fragment of a (5,5) SWCNT was used for all computational purposes. H atoms were used to cap the ends of this fragment, resulting in a system with molecular formula $C_{70}H_{20}$. One carbon atom in the middle of the SWCNT fragment was replaced with a Pt atom to give a symmetrical model system, $C_{69}H_{20}Pt$. DFT calculations were performed using the exchange-correlation density functional of Perdew, Burke, and Ernzerhof (PBEPBE).[63] Relativistic effects of the Pt atom were taken into account by the relativistic effective core pseudopotential of Hay and Wadt (LANL2).[64] We optimized the geometries of nanotube−adsorbate complexes with a number of small gases first for the monoadsorbed case using the LANL2MB basis set, which was subsequently refined with the LANL2DZ basis (Dunning/Huzinaga valence double-ζ for first-row elements and Los Alamos ECP plus double-ζ for heavier elements).[65] Our current computational resources do not allow us to further increase the size of basis set beyond LANL2DZ for such large systems.

In situations where multiple adsorption was examined, the optimized geometries of the monoadsorbed complex was taken as an initial point and a second molecule of the gas of interest was added in close vicinity of the Pt center with no restriction on symmetry. The same protocol was then used for geometry optimization. All optimized geometries are assumed to be minima without confirmation from vibrational frequency analyses, which require more computational resources than what we currently have. Natural bond orbital (NBO) analysis was carried out to estimate partial charges.[66,67] The Gaussian 03 quantum chemical package was used for all calculations.[68]

Previous work from our group has shown that spin-restricted and spin-unrestricted optimizations yield the same result for the same singlet species[38] and we hence treated all such systems with spin-unrestricted DFT. Furthermore, because of the presence of a low-lying triplet state for the bare Pt-doped SWCNT, singlet and triplet spin states were considered for all nanotube-adsorbate complexes where the gas existed in a ground-state singlet configuration. For investigations involving gases with unpaired electrons (ground-state doublet), doublet and quartet spin states were considered for the resulting nanotube-adsorbate complexes. Spin-unrestricted DFT was employed for all open-shell systems.

## 3. Results and Discussion

**3.1. Bare Pt-Doped SWCNTs.** We recently reported a full computational study on the geometry and electronic structures of bare Pt-doped SWCNT fragments capped with H atoms.[38] In agreement with related work regarding Pt-doped nanorods,[37] the H-capped fragments resulted in optimized geometries with the Pt atom occupying a position slightly outside the carbon wall of the tube (Figure 1a). The Pt center was bonded to three carbon atoms in a tripodal arrangement due to the larger atomic radius of Pt and longer Pt−C bonds.[38]

**TABLE 1: Binding Energy and Geometrical Data for Nanotube−Adsorbate Complexes with End-On Binding Motif**

| adsorbate | spin state | ΔE[a] | *d*(PtX)[b] | *d*(XY)[c] | *q*(Pt)[d] | *q*(XY)[e] | *q*(C)[f] |
|---|---|---|---|---|---|---|---|
| none[g] | singlet | 0 | N/A | N/A | 0.82 | N/A | −0.41 |
| | triplet | 0 | N/A | N/A | 0.84 | N/A | −0.49 |
| CO[g, h] | singlet | −41.23 | 1.97 | 1.19 | 0.85 | −0.12 | −0.43 |
| | triplet | −33.09 | 1.96 | 1.20 | 0.83 | −0.15 | −0.46 |
| OC[g, h] | singlet | −6.98 | 2.42 | 1.18 | 0.87 | −0.02 | −0.41 |
| | triplet | −6.78 | 2.35 | 1.19 | 0.88 | −0.06 | −0.45 |
| $(CO)_2$[g, h] | singlet | −73.67 | 2.00, 2.00 | 1.19, 1.19 | 0.83 | −0.05, −0.05 | −0.49 |
| | triplet | −58.95 | 2.00, 2.00 | 1.19, 1.19 | 0.78 | −0.02, −0.02 | −0.49 |
| $(CO)_3$[h] | singlet | −71.35 | 1.98, 2.00, 3.13 | 1.19, 1.19, 1.19 | 0.77 | 0.01, −0.01, −0.06 | −0.37 |
| | triplet | −73.74 | 2.03, 2.03, 2.41 | 1.18, 1.18, 1.19 | 0.76 | 0.05, 0.05, −0.13 | −0.46 |
| NO[h] | doublet-s | −46.97 | 1.91 | 1.24 | 0.99 | −0.39 | −0.39 |
| | doublet-t | −56.49 | 1.91 | 1.24 | 0.99 | −0.39 | −0.39 |
| | quartet | −46.17 | 2.00 | 1.25 | 0.95 | −0.38 | −0.34 |
| ON[h] | doublet-s | −23.18 | 2.14 | 1.27 | 0.98 | −0.37 | −0.34 |
| | doublet-t | −32.71 | 2.14 | 1.27 | 0.98 | −0.37 | −0.34 |
| | quartet | −29.99 | 2.12 | 1.29 | 1.00 | −0.44 | −0.33 |
| $(NO)_2$[h] | singlet | −69.94 | 2.10, 2.12 | 1.24, 1.24 | 0.99 | −0.24, −0.28 | −0.36 |
| | triplet | −77.75 | 2.12, 2.12 | 1.24, 1.24 | 0.99 | −0.25, −0.25 | −0.35 |
| $NH_3$[i] | singlet | −31.79 | 2.25 | N/A | 0.88 | 0.18 | −0.44 |
| | triplet | −31.28 | 2.23 | N/A | 0.87 | 0.18 | −0.50 |
| $(NH_3)_2$[i] | singlet | −57.10 | 2.27, 2.27 | N/A | 0.92 | 0.18, 0.18 | −0.48 |
| | triplet | −55.30 | 2.26, 2.26 | N/A | 0.86 | 0.19, 0.19 | −0.49 |
| $N_2$[j] | singlet | −24.72 | 2.08 | 1.16 | 0.91 | −0.14 | −0.41 |
| | triplet | −25.90 | 2.05 | 1.16 | 0.91 | −0.18 | −0.44 |
| $(N_2)_2$[j] | singlet | −43.91 | 2.16, 2.16 | 1.16, 1.16 | 0.93 | −0.09, −0.09 | −0.42 |
| | triplet | −41.68 | 2.16, 2.16 | 1.16, 1.16 | 0.89 | −0.09, −0.09 | −0.41 |

[a] Total stabilization energy (in kcal $mol^{-1}$). [b] Distance (in Å) between Pt and X of XY. [c] Distance (in Å) between X and Y of XY. [d] Partial charge on Pt. [e] Net partial charge on XY. [f] Net partial charge on the C atoms of the SWCNT adjacent to Pt. [g] Reference 38. [h] $(XY)_n$ refers to an *n* X-end adsorbed Pt-doped SWCNT fragment. [i] N-end adsorption. [j] End-on adsorption.

It is important to note that this model system represents only a fragment of a hypothetically infinite Pt-doped SWCNT. As mentioned above, the transition metal atoms present in the otherwise all-carbon backbone act as impurities in the nanotube itself. Since the model fragment displays this geometry where the Pt center points to the exterior of this supramolecular structure, it is highly possible that in the situation of random doping, the transition metal atoms may sufficiently backscatter carriers along the nanotube and lower the net conductivity instead of what was previously believed.[38] Further studies with periodic boundary conditions and much larger SWCNT segments may provide some insight into the true properties of this novel material.

**3.2. Adsorption of Carbon Monoxide.** The adsorption of CO onto an isolated Pt center was an obvious extension after identifying a geometry optimized structure of the bare Pt-doped SWCNT.[38] Indeed, the importance of CO to transition metals in general, both as discrete organometallic species and flat surfaces cannot be understated.[58,59,69−72] As this Pt-nanotube species represents a unique niche in between the extremes of isolated Pt centers stabilized by ligands and regular surfaces of Pt metal, we decided to continue our studies on the adsorption of CO.

Our previous work revealed that as in the case of classical alkylplatinum complexes, the adsorption of CO through the C atom is more energetically favorable than through the O atom (cf. 41.23 kcal $mol^{-1}$ for **C**O adsorption[73] vs 6.98 kcal $mol^{-1}$ for **O**C adsorption[73]).[38] The molecular orbitals that resulted from our calculations revealed that the simple molecular orbital description of CO was mostly sufficient; simply put, the lone pair of electrons on the C atom of CO donates into an appropriate unoccupied metal d orbital, which effectively stimulates the metal center to backdonate to the $\pi^*$ orbital of the adsorbate.[72,74,75] This **C**O-adsorbed Pt-doped SWCNT had an optimized geometry where the C≡O triple bond was elongated slightly from the bond length of the free gaseous molecule, in agreement with the simple picture described above (Figure 1b).[38] A net backdonation from the metal d orbitals results in a net charge of −0.12 on the adsorbed CO. Our preliminary studies showed a decrease in the HOMO−LUMO gap from 0.74 eV for the bare Pt-doped SWCNT to 0.58 eV in the case of ground state adsorption.

Our model study with alkylplatinum complexes of formulas $PtMe_3^{n+}$, however, suggested that more than one molecule of CO could be adsorbed onto the Pt center of the SWCNT.[38] Indeed, our attempt at geometry optimization where two molecules of CO bonded to the Pt atom was successful where the C-end orientation was used due to the favorable energetics of C-end adsorption versus O-end adsorption (vida supra). The structure of the $(\mathbf{C}O)_2$-adsorbed Pt-doped SWCNT fragment is shown in Figure 1d. The net energy released upon the second adsorption was only 73.67 kcal $mol^{-1}$, translating to an average of 36.83 kcal $mol^{-1}$ per molecule of CO (cf. 41.23 kcal $mol^{-1}$ for **C**O adsorption). This is most likely due to the increased steric hindrance about the transition metal center.[38]

In this case, both molecules are situated almost identically around the Pt atom, in an almost symmetric fashion. The distance between the adsorbate and the Pt center has now increased from 1.97 to 2.00 Å, suggesting an overall decrease in the interaction strength between the molecule of CO and the Pt-doped SWCNT itself. The backdonation has also diminished to −0.05 for each CO. Interestingly, the gap between the HOMO and the LUMO has reverted to 0.78 eV, within computational error of the bare Pt-doped SWCNT.[38]

Further efforts at determining optimized structures for the adsorption of three molecules of CO were initially thought to be futile, since the steric bulk of the carbon nanotube served as a large ligand that would hinder the adsorption of another adsorbate molecule.[38] Indeed, after repeated attempts, we were able to establish that while the Pt center alone could not bind three CO molecules, the assistance of the delocalized $\pi$-electrons

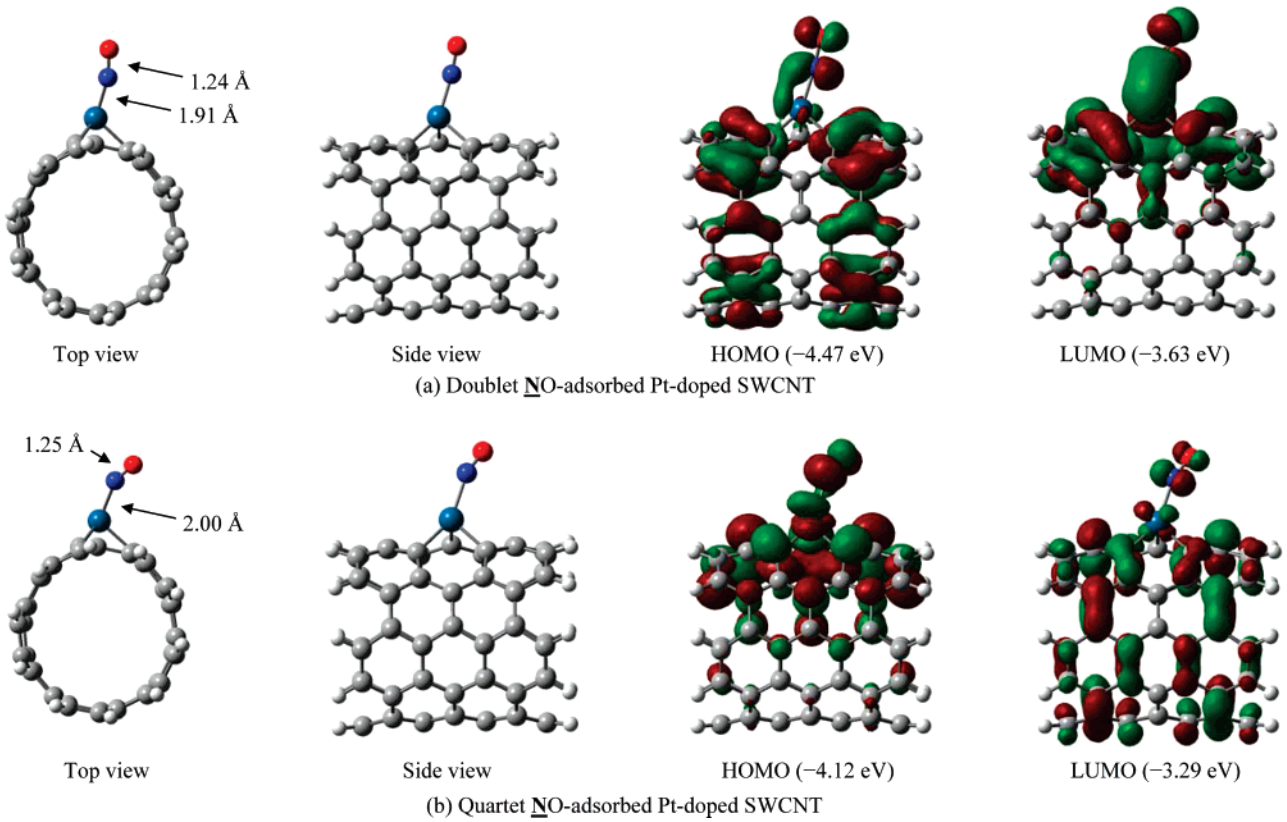


**Figure 3.** Doublet and quartet NO-adsorbed Pt-doped SWCNTs. The numbers in parentheses are the orbital energies in eV.

along the backbone of the nanotube could make this possible (Figures 1e and 2).

This transformation is exothermic relative to the bare Pt-doped SWCNT but requires an input of energy from the doubly adsorbed system. The geometry here bears great similarity to that of the $(CO)_2$-adsorbed Pt-doped SWCNT where C-end adsorption of CO takes place, for both the singlet and triplet spin states. However, the orientation of the third molecule of CO is an interesting one, as it appears that a weaker interaction takes place between the Pt d orbitals and the $\pi$-system of the adsorbate (3.13 Å between the Pt atom and the C atom of the third CO, compared to 1.97 and 2.00 Å for the other two molecules of CO for the singlet).

An NBO analysis reveals that the partial charge on the Pt center is 0.77, while the net charge on the two CO molecules directed at the metal atom bear charges of 0.01 and −0.01, respectively. The third molecule of CO, which also interacts with the carbon backbone, exhibits a charge of −0.06. This suggests that the majority of the backdonation from the Pt atom is to the third molecule of CO. The electron configuration of the Pt center is essentially $[Xe]6s^{0.49}5d^{8.72}$ and the HOMO−LUMO gap has again decreased to 0.52 eV.

Detailed structural and binding energy data for nanotube-adsorbate complexes with end-on binding motif are collected in Table 1.

**3.3. Adsorption of Nitrogen Monoxide.** Our investigation of CO as an adsorbate for Pt-doped SWCNTs naturally suggested an extension involving nitrogen monoxide. Unlike CO, NO is a ground state doublet, bearing a single unpaired electron. The adsorption of NO on Pt surfaces has been previously investigated[76−82] and it appears that chemisorption often results in molecular dissociation.[76] NO appears to have less utility as a ligand than CO but has been shown to interact with metal centers (note that NO, a radical, is distinct from $NO^+$ and $NO^-$ ligands that are prevalent in organometallic chemistry).[83,84]

Since free NO exists in a doublet state, spin selection rules limit an NO-adsorbed Pt-doped SWCNT species to either doublet or quartet states (ignoring higher energy excitations). Beginning with a singlet ground state nanotube, a doublet state can be achieved via reaction with doublet NO (no net change in spin). However, if the starting point is instead a triplet Pt-doped nanotube segment, both doublet and quartet final states can be accessed. Herein, we will refer to the doublet state resulting from the singlet Pt-doped SWCNT as doublet-s and the alternative from a triplet initial configuration as doublet-t.

Like in the case of CO adsorption, we began our investigation by considering the obvious possibility of binding through the N atom. In this case, formation of the doublet-s state results in the liberation of −46.97 kcal $mol^{-1}$, while the doublet-t state is −56.49 kcal $mol^{-1}$ below the triplet Pt-doped SWCNT. Finally, −46.17 kcal $mol^{-1}$ is released for the quartet state. Geometrically, we observe similar effects of adsorption on the adsorbate (Figures 1f and 3). In particular, the NO separation is 1.24 Å in the doublet and 1.25 Å in the quartet (cf. 1.21 Å for the free gas), while the distance to the Pt center is 1.91 and 2.00 Å for these two spin states, respectively. The Pt−N−O bond angles are 165° and 152° for the doublet and quartet NO-adsorbed Pt-doped SWCNT, respectively. Qualitatively, it appears that there is a slightly smaller interaction between the adsorbed NO and the Pt-doped SWCNT in the quartet case than in the doublet case.

For the doublet, the Pt atom now bears a charge of 0.99, while the N atom exhibits a net charge of −0.21 and the O atom has a −0.18 charge. In comparison, the quartet system shows a Pt center with charge 0.95 and the N and O atoms

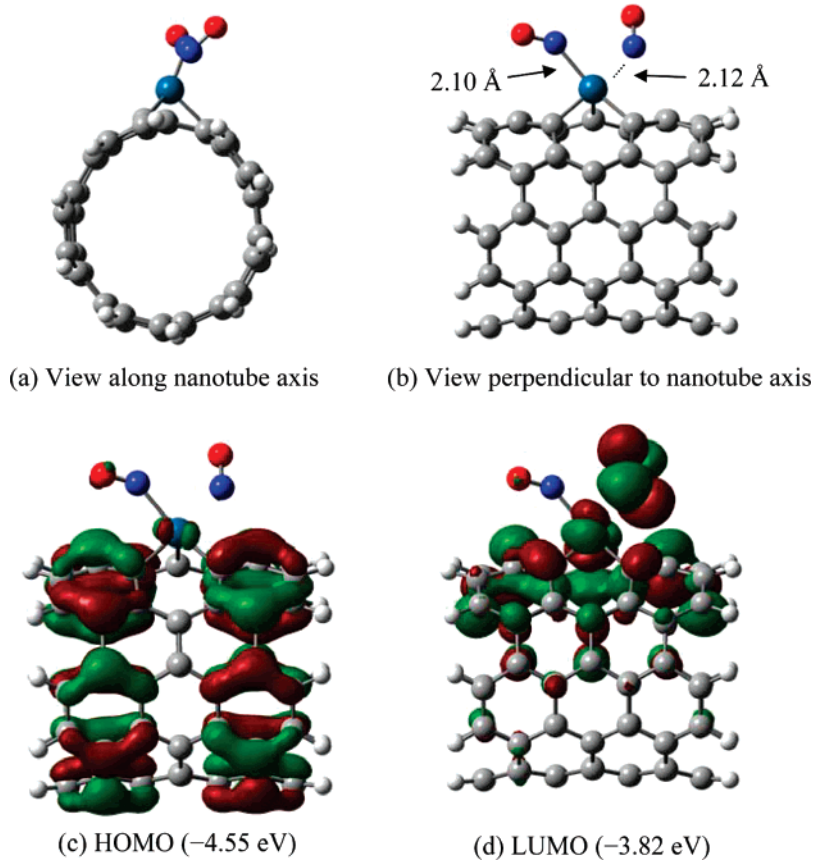


**Figure 4.** Ground state (NO)$_2$-adsorbed Pt-doped SWCNT. The numbers in parentheses are the orbital energies in eV.

nearby bearing −0.17 and −0.20 charges, respectively. The electronic configuration of the Pt atom is [Xe]6s$^{0.45}$5d$^{8.55}$ in the case of the doublet and [Xe]6s$^{0.42}$5d$^{8.62}$ for the quartet. Overall, it is interesting to note that in comparison to the effect of CO adsorption, the electronic structure of the entire supramolecular entity is altered to a greater extent from the bare Pt-doped SWCNT (HOMO−LUMO gap of 0.84 eV for the doublet, 0.83 eV for the quartet). Clearly, the unpaired electron on the NO molecule plays a significant role.

The unsymmetrical arrangement of atoms (Figure 3) between the two spin states is also of interest and suggests a difference in the type of interactions between the N atom and the metal center. Carter and co-workers[84] reported a computational study of transition metals attached to simple gases including CO and NO. It was found that the ground state complex formed between a Pt center and NO is $^2$A', with the atoms arranged in a bent fashion. Here, a strong $\sigma$-bond is formed between a Pt d$\sigma$ orbital and the N $\pi$* orbital. The first excited state, however, has term symbol $^2\Sigma^+$, and the major interaction is between the d$\pi$ orbital of the Pt atom and the $\pi$* orbital of NO.[84] Our results differ from those reported for the isolated Pt atoms, as we have already shown that the steric bulk of the nanotube (which acts like a ligand)[38] plays an important role in the binding of small molecules on the Pt center for Pt-doped SWCNTs. In this case, the doublet ground state is closer to a linear geometry than the more bent quartet excited state (which follows from the work of Carter) as steric crowding increases the energy of the bent configuration. Electronic factors also likely play a role, as the delocalization of electron density that is possible for the nanotubes but not for the isolated atoms should favor the $\sigma$-donation of the lone pair of electrons residing on the N atom along the axis of the adsorbed NO molecule.

As in the CO case, we must also consider the alternative: adsorption through the O atom. Geometry optimization gave a reasonable structure where a weaker Pt−O interaction was found (Figure 1g), and the O-end adsorbed NO expels less energy upon adsorption. The formation of doublet-s results in the liberation of −23.18 kcal mol$^{-1}$, while that for doublet-t and quartet spin states are −32.71 and −29.99 kcal mol$^{-1}$, respectively. Because of the weaker interaction between NO and the Pt-doped SWCNT, the distance from the Pt center to the adsorbate is increased from 1.91 Å in the case of N-end adsorption to 2.14 Å for O-end adsorption. HOMO−LUMO gaps for the doublet and quartet states are 0.84 and 0.83 eV, respectively.

The possibility of multiple adsorption was also of interest, especially for comparison to the (CO)$_2$-adsorbed system. For simplicity, we considered only double adsorptions where the N atom was the biting end. While we might expect equivalent interaction between both molecules of NO and the Pt atom, this was not the case for the ground state (NO)$_2$-adsorbed Pt-doped SWCNT (Figures 1h and 4). Instead, we found a geometry where the O atom on one of the NO molecules points away from the nanotube surface. This suggests that again, the steric bulk of the C atoms along the nanotube backbone play a significant role on the adsorption geometry of small molecules, especially in regards to the interaction between adsorbates and the $\pi$ system itself. Interestingly, the triplet excited-state showed a different arrangement of atoms, a symmetrical one as predicted by analogy to (CO)$_2$-adsorbed Pt-doped SWCNTs.[38]

Finally, since the adsorption of three molecules of CO was shown to be dependent on the surface of the SWCNT itself, we did not consider the case where three NO molecules adsorb onto the Pt center.

**3.4. Adsorption of Ammonia.** Ammonia, $NH_3$, is a common stabilizing ligand found in a number of Pt complexes and has been a wide area of investigation.[85−89] For example, the first antitumor agent containing a transition metal was cisplatin, a molecule of formula $Cl_2Pt(NH_3)_2$, where $NH_3$ acts as a stabilizing ligand for the Pt center.[90] At the other extreme, heterogeneous Pt surfaces and their interaction with $NH_3$ is vital to an industrial process whereby $NH_3$ is oxidized to NO.[91] Hence, the adsorption characteristics of $NH_3$ on Pt are of great significance and has been studied in great detail for a number of similar systems.[92−96]

As a ligand, $NH_3$ is dramatically different than both CO and NO. Because of the absence of a low-lying $\pi^*$ orbital that is easily accessible for both CO and NO, backbonding from metal d orbitals is not generally invoked in a simple molecular orbital description of the metal−ligand bonding. Instead, the main interaction between $NH_3$ and any transition metal is likely the donation of electrons from the ligand to the metal in a $\sigma$-bonding fashion.[72]

The optimized geometries for singlet and triplet $\underline{\mathbf{N}}H_3$-adsorbed Pt-doped SWCNTs are shown in Figure 1i. The adsorption energies in this case are −31.79 and −31.28 kcal mol$^{-1}$ for singlet and triplet states, respectively, with corresponding HOMO−LUMO gaps of 0.73 and 0.39 eV. The adsorption, however, appears to be weaker in comparison to CO and NO: $d$(PtN) = 2.25 Å for singlet ground state, 2.23 Å for triplet excited state. The interaction takes place with an unsymmetrical geometry, similar to that observed for CO and NO adsorption cases.

Accessing our calculation with NBO analysis, we found that the charge residing on the Pt center was 0.88, −1.13 on the N atom, and approximately 0.44 on each of the H atoms in $NH_3$. This suggests that there is an overall donation of the electrons from $NH_3$ to the Pt-doped SWCNT, unlike the backdonation that was observed for CO and NO adsorbates. This is not unexpected, as the $\sigma^*$ orbital of $NH_3$ is of much higher energy than the $\pi^*$ orbital of CO and NO, minimizing orbital interactions and charge transfer from the nanotube to the $NH_3$ gas. The electronic configuration about the Pt atom is essentially $[Xe]6s^{0.46}5d^{8.67}$.

The adsorption of two molecules of $NH_3$ was also considered and optimized geometries (Figure 1j) gave energies of −57.10 kcal mol$^{-1}$ for the singlet $(\underline{\mathbf{N}}H_3)_2$-adsorbed Pt-doped SWCNT and −55.30 kcal mol$^{-1}$ for the corresponding triplet species. Again, the average energy released per molecule of $NH_3$ is decreased because the steric clash between two adsorbates increases the energetics of a doubly bound complex. The net charge on the $NH_3$ is almost unchanged at 0.18 for the singlet and 0.19 for the triplet. The HOMO−LUMO gap is increased to 0.75 eV for the singlet and reduced to a mere 0.25 eV in the case of the triplet.

Three molecules of $NH_3$ were not considered for the purposes of this study.

**3.5. Adsorption of Nitrogen Gas.** Up until this point, all proposed analytes that act as ligands for the metal center in Pt-doped SWCNTs have been polar. The inherent polarity of small gases facilitates their interaction by directing their electron density to the metal center. In reality, however, not all gases exhibit a natural polarity and it is thus important to consider the interaction between the Pt center on this nanotube and nonpolar gases such as $N_2$.

$N_2$, in particular, has been the focus of many groups across the world due to its importance in the biologically relevant nitrogen cycle and also in the industry as a feedstock for the Haber-Bosch production of $NH_3$.[72] In particular, transition metal-mediated activation of $N_2$ is of interest because the natural process of nitrogen fixation is carried out by a number of bacteria containing FeMo metalloenzymes[97] or alternative nitrogenases employing vanadium as the active metal center.[98] The first transition metal complex shown to interact with an otherwise inert $N_2$ gas[99] was $[Ru(NH_3)_5(N_2)]^{2+}$, isolated in 1965.[100]

The activation of $N_2$ generally takes place through two possible mechanisms. First, $N_2$ can bind in an end-on fashion, acting as a $\sigma$-donor to the metal and accepting electrons from the metal into a $\pi^*$ orbital. In this scenario, the transition metal is typically low valent and bears an open-coordination site that is accessible almost exclusively to the small $N_2$ molecule.[101] This type of interaction requires highly active metal centers because unlike their isoelectronic analogues CO and $NO^+$, $N_2$ is a fairly poor ligand due to equal atomic contributions from each N atom.[72,99] However, a second mode of binding exists for $N_2$, where side-on binding can take place. In these circumstances, $N_2$ coordinates to two metal centers, typically lanthanides and actinides, although a number of other transition metals have been shown to bind to $N_2$ in an $\eta^2$-motif.[99]

We considered both possibilities and attempt to optimize geometries for an $N_2$-adsorbed Pt-doped SWCNT species. It was to our surprise that regardless of our starting point, optimization ultimately gave a structure where $N_2$ was coordinated in an end-on fashion (Figure 1k). As expected, the geometry is not too different from that of CO, but the energetics are clearly not the same. Stabilization as a result of $N_2$ adsorption onto the Pt center is only −24.72 kcal mol$^{-1}$ for the singlet and −25.90 kcal mol$^{-1}$ for the triplet (cf. −41.03 kcal mol$^{-1}$ for the singlet $\underline{\mathbf{C}}$O-adsorbed Pt-doped SWCNT and −33.09 kcal mol$^{-1}$ for the triplet). Again, with the loss of natural polarity in the adsorbate, this decrease is not unexpected. Geometrically, the N≡N separation is lengthened slightly from 1.15 Å in the free gas to 1.16 Å in the $N_2$-adsorbed Pt-doped SWCNT fragments.

The net charge on the $N_2$ molecule is −0.14 and −0.18 for the singlet and triplet states, respectively. This implies that while the interaction between the Pt center and the $N_2$ molecule may be weak, there is sufficient orbital overlap so that electron density can flow out of the Pt-doped SWCNT and into the oncoming ligand. The electronic configuration of the Pt center is $[Xe]6s^{0.45}5d^{8.63}$ for the singlet and $[Xe]6s^{0.42}5d^{8.66}$ for the triplet. This suggests that the Pt atom is relatively electropositive and able to activate even nonpolar molecules such as $N_2$.

Completely analogous to CO and NO adsorptions, the multiple adsorption of $N_2$ was considered. Here, since both side-on and end-on starting points gave an optimized geometry where end-on binding was observed, we opted to explore only $(N_2)_2$-adsorbed Pt-doped SWCNT structures where both adsorbates were oriented with one end toward the metal center (Figure 1l). Unlike previous cases, however, the adsorption energy of each molecule of $N_2$ is not significantly lower than that of the singly adsorbed scenario (−43.91 kcal mol$^{-1}$ total for ground state double adsorption vs −24.72 kcal mol$^{-1}$ for ground state single adsorption). It is quite possible that the weaker interaction between the Pt center and the N $\sigma$ orbitals results in a longer coordinate bond and gives a lower steric repulsion between the two molecules of $N_2$ attached to the same metal atom. As a result, the total energy of adsorption for two molecules of $N_2$ is quite close to twice the amount of energy released for the binding of a single molecule of $N_2$. The HOMO−LUMO gap

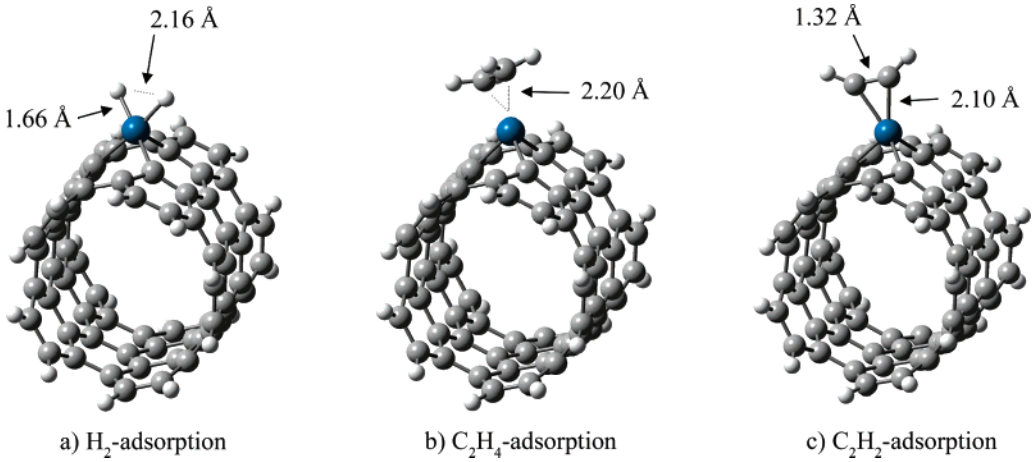


**Figure 5.** Optimized geometries of side-on adsorbed Pt-doped SWCNT fragments.

for the singlet state of this double adsorption is 0.81 eV, compared to 0.63 eV for the triplet state.

**3.6. Adsorption of Hydrogen Gas.** With the examination of $N_2$ adsorption behind us, we now turn our attention to species that selectively bind to metal centers in a side-on fashion, the simplest of which is $H_2$. The activation of $H_2$ on Pt surfaces has found application in numerous synthetic organic sequences where the hydrogenation of alkenes and alkynes can be achieved through heterogeneous catalysis.[102] Advances then pushed toward catalytic reactions involving $H_2$ using well-defined organometallic complexes (e.g., Wilkinson's catalyst)[72] and ultimately asymmetric versions of the reaction as pioneered by Knowles[103] and by Kagan and Dang.[104] Again, our Pt-doped SWCNT sits uniquely in between the two extremes of heterogeneous and homogeneous activation of small molecules.

We were able to identify optimized geometry for the adsorption of $H_2$ onto Pt-doped SWCNTs (Figure 5a). In agreement with a computational study conducted from our group earlier on Pt-doped SWCNT fragments capped with hemispherical fullerene-like structures, the interaction is a chemisorption process.[37] In other words, the net result is the cleavage of the H−H bond. The energetic preference for this reaction was determined to be −11.32 and −6.02 kcal mol$^{-1}$ for singlet and triplet states, respectively. The gap between the HOMO and the LUMO is 0.70 eV for the ground state and 0.39 eV for the excited state. The distance between the two H atoms is elongated from 0.75 Å to a surprising 2.16 Å for the singlet $H_2$-adsorbed Pt-doped SWCNT species as a result of electron transfer from the $\sigma$ orbital of $H_2$ to the empty 5d orbital of the Pt center. The Pt−H distance is ca. 1.66 Å for both spin states.

The chemisorption process represents a formal oxidative addition, where the oxidation state of the Pt atom has increased by two, as in the case for classical transition metal-based hydrogenation catalysts.[72] This suggests that individual molecules of $H_2$ can adsorb individually onto each Pt center on an infinitely long Pt-doped SWCNT. While the exact mechanism of adsorption has not been studied here, it is reasonable to expect that since the process of adsorption is only mildly exothermic, the $H_2$-adsorbed state should be favored at low temperatures, while a bare state should be the predominant species at higher temperature. Hence, the adsorption and desorption of $H_2$ from the Pt-doped SWCNT should be easily reversible. It is interesting to note that the selective doping of Pt onto the backbone of SWCNTs may provide the overall surface with an enhanced ability to interact with $H_2$, thus improving its ability as a hydrogen storage device. In fact, since the report of Dillon et al. in 1997,[105] the interest in using carbon nanotubes as a means of storing hydrogen has skyrocketed. The key advantage to a Pt-doped SWCNT (or doping with any transition metal, for that fact) is that instead of being limited to the relatively weak interaction with the extremely large surface area of a nanotube,[105] metal atoms allow for direct activation. While the metal-doped SWCNT has not yet been realized, one of its first potential applications could thus be as an improved carbon-based hydrogen storage material.

The net charge on the Pt center as a result of $H_2$ adsorption is 0.77 for the singlet and 0.74 for the triplet. On the adsorbate itself, an overall charge of −0.34 was determined for both spin states. The electronic configuration of the Pt center is essentially [Xe]6s$^{0.57}$5d$^{8.64}$ and [Xe]6s$^{0.57}$5d$^{8.68}$ for the ground and excited states, respectively.

Detailed structural and binding energy data for nanotube-adsorbate complexes with side-on binding motif are summarized in Table 2.

**3.7. Adsorption of Ethylene.** As in the case of $H_2$, the simplest two carbon alkene with molecular formula $C_2H_4$ known as ethene or ethylene has been of great interest, particularly to catalytic hydrogenation.[106] In general, alkenes have been found to undergo a rehybridization on transition metal surfaces to a doubly $\sigma$-bonded complex, where a three-membered metallocyclopropane is formed.[107] As opposed to this chemisorption-type interaction, a simple coordination can also take place, where the $\pi$ electrons interact with a metal center, as is the case for many organometallic complexes.[72]

The geometry optimized structure (Figure 5b), again with agreement with our previous work involving Pt-doped nanorods, revealed that a molecule of $C_2H_4$ can interact with isolated Pt centers protruding to the exterior of the carbon backbone via physisorption.[37] The release of energy coming from the physisorption is appropriately smaller than for most adsorption processes (Table 1), with values of −26.43 kcal mol$^{-1}$ for the singlet Pt-doped SWCNT and −24.74 kcal mol$^{-1}$ for corresponding triplet state. The values for the HOMO−LUMO gap for these spin states are 0.88 and 0.62 eV, respectively. The C═C bond is elongated from 1.35 to 1.43 Å upon the adsorption of the molecule of ethylene onto the Pt atom and the distance between the Pt atom and either C atom of $C_2H_4$ is approximately 2.30 Å.

The interaction can be thought to take place through $\pi$ donation of the alkene to an empty d orbital of the metal.[72] It is interesting to note that despite this relatively weak adsorption process, there is still significant donation of electrons from the

**TABLE 2: Binding Energy and Geometrical Data for Nanotube−Adsorbate Complexes with Side-On Binding Motif**

| adsorbate | X | spin state | $\Delta E^a$ | $d(PtX)^b$ | $d(XX)^c$ | $q(Pt)^d$ | $q(X_2)^e$ | $q(C)^f$ |
|---|---|---|---|---|---|---|---|---|
| none[g] | N/A | singlet | 0 | N/A | N/A | 0.82 | N/A | −0.41 |
| | N/A | triplet | 0 | N/A | N/A | 0.84 | N/A | −0.49 |
| $H_2$ | H | singlet | −11.32 | 1.66, 1.68 | 2.16 | 0.77 | −0.34 | −0.33 |
| | H | triplet | −6.02 | 1.66, 1.66 | 2.19 | 0.74 | −0.34 | −0.43 |
| $C_2H_4$ | $CH_2$ | singlet | −26.43 | 2.31, 2.20 | 1.43 | 0.95 | −0.25 | −0.35 |
| | $CH_2$ | triplet | −24.74 | 2.31, 2.30 | 1.42 | 0.92 | −0.16 | −0.37 |
| $C_2H_2$ | CH | singlet | −31.36 | 2.13, 2.10 | 1.32 | 0.98 | −0.38 | −0.34 |
| | CH | triplet | −25.29 | 2.17, 2.15 | 1.30 | 0.92 | −0.27 | −0.31 |

[a] Total stabilization energy (in kcal $mol^{-1}$). [b] Distances (in Å) between Pt and each X of $X_2$. [c] Distance (in Å) between X and X of $X_2$. [d] Partial charge on Pt. [e] Net partial charge on $X_2$. [f] Net partial charge on the C atoms of the SWCNT adjacent to Pt. [g] Reference 38.

Pt-doped SWCNT onto the gas, −0.25 for the singlet and −0.16 for the triplet, similar to that observed for $N_2$ adsorption (vide supra).

**3.8. Adsorption of Acetylene.** Similar to ethylene, the two carbon alkyne, $C_2H_2$, known as ethyne or acetylene is of significance to the chemical industry in matters of hydrogenation as catalyzed by Pt surfaces.[61,62] In fact, the interaction between acetylene and Pt is often so strong that it is readily converted into ethane instead of terminating at ethylene.[62,108,109] In traditional organometallic chemistry, the utility of alkynes as ligands is also an important area of investigation.[72] Complexes range from species where the alkyne acts simply as a $\pi$-donor to a metal to a more significant interaction where the transition metal has undergone an oxidative addition, yielding a metallocyclopropene.[72]

In comparison to the free acetylene C≡C distance (1.23 Å), the geometry optimized structure of the $C_2H_2$-adsorbed Pt-doped SWCNT (Figure 5c) has bond distances of 1.32 and 1.30 Å for singlet and triplet states, respectively. The adsorption is again exothermic, liberating −31.36 kcal $mol^{-1}$ for the singlet ground state configuration and −25.29 kcal $mol^{-1}$ for the triplet excited state. The separation between the HOMO and the LUMO is 0.88 eV for the singlet spin state and 0.60 eV for the triplet. The distance between the Pt atom and either C atom of acetylene is approximately 2.15 Å. Clearly, there is substantial interaction between the adsorbate and the metal atom, approaching that of a metallocyclopropene-type structure (i.e., chemisorption).[72] By taking a closer look at the geometry, it becomes evident that the C−H bonds of the acetylene exhibit substantial bending, approximately at 150° for either spin state (cf. 180° in the free molecule). This suggests that the adsorption changes the hybridization of the two C atoms of $C_2H_2$ from sp to almost $sp^2$.

Calculations reveal that the $C_2H_2$-adsorbed Pt-doped SWCNT has Pt centers with charges 0.98 and 0.92 for the singlet and triplet states, respectively. The backdonation from the nanotube to the adsorbate is −0.38 for ground state and −0.27 for the excited state. Interestingly, this charge transfer is quite similar to that determined for the chemisorption of $H_2$. The Pt center has electronic configuration $[Xe]6s^{0.41}5d^{8.60}$ for the singlet and $[Xe]6s^{0.43}5d^{8.65}$ for the triplet.

**3.9. Application as Gas Sensors.** Each geometry optimized structure determined above represents a case study of how the electronic properties of a Pt-doped SWCNT might be affected by the presence of small gas molecules. In particular, the sensitivity can be evaluated by two parameters: first, the charge transfer from the supramolecular framework to the analyte[51] and, second, by the HOMO−LUMO gap of the system.[38] In essence, the donation of electron density from the nanotube to the adsorbate results in a change in conductance of the nanotube.[51,55,56] This, in turn, is driven by a realignment of chemical potential of the combined nanotube-adsorbate complex.[51] The sensitivity is hence correlated to the value of the charge transfer by the following equation:[51]

$$\Delta Q = C_g \Delta V_g = \partial\theta \frac{\pi d l}{\sigma} \quad (1)$$

where the transferred charge, $\Delta Q$, is directly proportional to the capacitance of the device, $C_g$, and the observed voltage change, $\Delta V_g$. Here, the parameters $d$ and $l$ are specific to the nanotube, representing the nanotube diameter and length, respectively, while $\sigma$ and $\theta$ are specific to the adsorbate, representing the molecular cross-section area and coverage, respectively.[51]

**TABLE 3: Charge Transfer and HOMO−LUMO Gap Data for Nanotube−Adsorbate Complexes with Side-On Binding Motif**

| analyte | average charge transfer[a] | HOMO−LUMO gap (eV) |
|---|---|---|
| none[b] | N/A | 0.74 |
| CO[c] | 0.05 | 0.78 |
| NO[d] | 0.28 | 0.74 |
| $NH_3$[e] | −0.18 | 0.75 |
| $N_2$[f] | 0.09 | 0.81 |
| $H_2$ | 0.34 | 0.70 |
| $C_2H_4$ | 0.25 | 0.88 |
| $C_2H_2$ | 0.38 | 0.88 |

[a] Represents charge donated from the Pt-doped SWCNT to the adsorbate. [b] Reference 38. [c] Represents $(\underline{C}O)_2$-adsorbed Pt-doped SWCNT. [d] Represents $(\underline{N}O)_2$-adsorbed Pt-doped SWCNT. [e] Represents $(\underline{N}H_3)_2$-adsorbed Pt-doped SWCNT. [f] Represents $(N_2)_2$-adsorbed Pt-doped SWCN T.

Our investigations revealed that the Pt-doped SWCNT is quite appropriate as a gas sensor in comparison to the undoped pure SWCNT (Table 3). For simplicity, we will only consider the scenario where the thermodynamic complexes are the products of the gas adsorption (i.e., the ground state configuration with the lowest energy orientation of adsorbates).

Table 3 clearly shows that for almost all of the species examined for Pt-doped SWCNTs there is a net charge transfer from the nanotube to the analyte. This is not unexpected, as the binding of a ligand to a metal is often associated with the backdonating of electrons from the metal to the ligand.[72] The net donation of $NH_3$ to the supramolecular framework is also understandable, because any backdonation from the nanotube would necessarily fill the LUMO, which is a high energy $\sigma^*$ orbital for $NH_3$, unlike the lower-lying $\pi^*$ orbitals of the other gases studied. The magnitude, however, seems appropriate for detection limits (the maximum charge transfer observed for a similar study involving B- and N-substitutionally doped SWCNTs was −0.28[51]).

Furthermore, the HOMO−LUMO gap is related to the ease in exciting an electron from the valence band of the material to the conduction band, although the correlation may not be a direct one. In this case, it is also apparent that changes in conductivity should be observed as a result of the adsorption of small gas molecules. While the change in HOMO−LUMO gaps as a result of adsorption onto a Pt center does not appear significant, the effect is expected to be greatly enhanced when we consider the nanotube as a whole with many adsorption sites. We are hopeful that the combined effect of many Pt atoms will allow for the design of a device that can detect gases at sub-ppm concentrations.[51]

The situation obviously becomes more complicated if the triplet state of the Pt-doped SWCNT is mixed in with the singlet state and excited states of the nanotube-adsorbate complexes also become accessible. However, this challenge ultimately lies in the synthesis or selective excitation of transition-metal doped nanotubes. For simplicity, we will not indulge on this topic at this moment.

On another note, while we could potentially use metal-doped nanotubes as sensors, there is also a potential application in nanoelectronics. Consider for a moment a nanodevice where a Pt-doped SWCNT acts as a wire or resistor. In this case, exposure to a gas such as CO or $H_2$ will result in a charge transfer from the nanotube to the adsorbate. As a result, the gate capacitance of the wire or resistor changes.[51] While further studies are necessary to illustrate the reversibility of the binding process, reducing the ambient pressure and changing the temperature around the Pt-doped SWCNT might allow for the removal of these small molecules. Potentially, the adsorption of gases onto these supramolecular structures would give us a method of reversibly modifying the electronics of the nanotube, a very appealing asset to this proposed material.

## 4. Conclusion

The adsorption of small molecules on a transition-metal doped SWCNT has been studied extensively within density functional theory. By replacing a C atom with a Pt atom on the SWCNT backbone, we have shown that the adsorption of gases is favorable and results in a charge-transfer event that modifies the conductance of the nanotube as a whole. By exposing a Pt-doped SWCNT to a variety of gases, we envision an application of this proposed material in both sensory technology and nanoelectronics. We believe that such initial investigations should provide experimentalists with a first look into the chemical and physical properties of these new materials and will further encourage continual research in this field in the years to come.

**Acknowledgment.** We acknowledge financial support from the Natural Sciences and Engineering Research Council (NSERC) of Canada for financial support. WestGrid and C-HORSE have provided the necessary computational resources. C.S.Y. thanks NSERC for an Undergraduate Student Research Award. L.V.L. recognizes the University of British Columbia for financial support in the form of a Gladys Estella Laid Fellowship and a Charles A. McDowell Fellowship.

**Supporting Information Available:** Optimized geometries (Cartesian coordinates) of all ground state nanotube-adsorbate complexes within the full DFT scheme and full citation for ref 68. This information is available free of charge via the Internet at http://pubs.acs.org.

## References and Notes

(1) Iijima, S.; Ichihashi, T. *Nature* **1993**, *363*, 603.
(2) Chen, Z.; Appenzeller, J.; Lin, Y.-M.; Sippel-Oakley, J.; Rinzler, A. G.; Tang, J.; Wind, S. J.; Solomon, P. M.; Avouris, P. *Science* **2006**, *311*, 1735.
(3) Singh, K. V.; Pandey, R. R.; Wang, X.; Lake, R.; Ozkan, C. S.; Wang, K.; Ozkan, M. *Carbon* **2006**, *44*, 1730.
(4) Lastella, S.; Mallick, G.; Woo, R.; Karna, S. P.; Rider, D. A.; Manners, I.; Jung, Y. J.; Ryu, C. Y.; Ajayan, P. M. *J. Appl. Phys.* **2006**, *99*, 024302.
(5) Byon, H. R.; Choi, H. C. *J. Am. Chem. Soc.* **2006**, *128*, 2188.
(6) Ferrer-Anglada, N.; Gomis, V.; El-Hachemi, Z.; Weglikovska, U. D.; Kaempgen, M.; Roth, S. *Phys. Stat. Solid.* **2006**, *203*, 1082.
(7) Liu, C.; Tong, Y.; Cheng, H.-M.; Golberg, D.; Bando, Y. *Appl. Phys. Lett.* **2005**, *86*, 223114.
(8) Jung, M.-S.; Ko, Y. K.; Jung, D.-H.; Choi, D. H.; Jung, H.-T.; Heo, J. N.; Sohn, B. H.; Jin, Y. W.; Kim, J. *Appl. Phys. Lett.* **2005**, *87*, 013114.
(9) Britz, D. A.; Khlobystov, A. N. *Chem. Soc. Rev.* **2006**, *35*, 637.
(10) Yeo-Heung, Y.; Miskin, A.; Kang, P.; Jain, S.; Narasimhadevara, S.; Hurd, D.; Shinde, V.; Schulz, M. J.; Shanov, V.; He, P.; Boerio, F. J.; Shi, D.; Srivinas, S. *J. Intel. Mater. Sys. Struc.* **2006**, *17*, 107.
(11) Li, C.; Chou, T.-W. *J. Intel. Mater. Sys. Struc.* **2006**, *17*, 247.
(12) Yun, Y.-H.; Shanov, V.; Schulz, M. J.; Narasimhadevara, S.; Subramaniam, S.; Hurd, D.; Boerio, F. J. *Smart Mater. Struc.* **2005**, *14*, 1526.
(13) Landi, B. J.; Raffaelle, R. P.; Heben, M. J.; Alleman, J. L.; VanDerveer, W.; Gennett, T. *Mater. Sci. Eng. B* **2005**, *116*, 359.
(14) Nakazawa, M.; Nakahara, S.; Hirooka, T.; Yoshida, M.; Kaino, T.; Komatsu, K. *Opt. Lett.* **2006**, *31*, 915.
(15) Seo, J.; Ma, S.; Yang, Q.; Creekmore, L.; Battle, R.; Tabibi, M.; Brown, H.; Jackson, A.; Skyles, T.; Tabibi, B.; Jung, S.; Namkung, M. *J. Phys.: Conf. Ser.* **2006**, *38*, 37.
(16) Sakakibara, Y.; Rozhin, A. G.; Kataura, H.; Achiba, Y.; Tokumoto, M. *Jap. J. Appl. Phys.* **2005**, *44*, 1621.
(17) Set, S. Y.; Yaguchi, H.; Tanaka, Y.; Jablonski, M. *J. Lightwave Technol.* **2004**, *22*, 51.
(18) Rozhin, A. G.; Sakakibara, Y.; Tokumoto, M.; Kataura, H.; Achiba, Y. *Thin Solid Films* **2004**, *464*−*465*, 368.
(19) Wu, D. H.; Chien, W. T.; Chen, C. S.; Chen, H. H. *Sens. Actuators A: Phys.* **2006**, *126*, 117.
(20) Kim, J.; Baek, J.; Kim, H.; Lee, K.; Lee, S. *Sens. Act. A* **2006**, *128*, 7.
(21) Kose, M. E.; Harruff, B. A.; Lin, Y.; Veca, L. M.; Lu, F.; Sun, Y.-P. *J. Phys. Chem. B* **2006**, *110*, 14032.
(22) Jeng, E. S.; Moll, A. E.; Roy, A. C.; Gastala, J. B.; Strano, M. S. *Nano Lett.* **2006**, *6*, 371.
(23) Wongwiriyapan, W.; Honda, S.-I.; Konishi, H.; Mizuta, T.; Ikuno, T.; Ito, T.; Maekawa, T.; Suzuki, K.; Ishikawa, H.; Oura, K.; Katayama, M. *Jap. J. Appl. Phys.* **2005**, *44*, L482.
(24) Liu, J.; Tian, S.; Knoll, W. *Langmuir* **2005**, *21*, 5596.
(25) Zhang, H. *J. Nanoparticle Res.* **2004**, *6*, 665.
(26) Hamada, N.; Sawada, S.-i.; Oshiyama, A. *Phys. Rev. Lett.* **1992**, *68*, 1579.
(27) Liu, L. V.; Tian, W. Q.; Wang, Y. A. *J. Phys. Chem. B* **2006**, *110*, 1999.
(28) Zhang, G.; Qi, P.; Wang, X.; Lu, Y.; Mann, D.; Li, X.; Dai, H. *J. Am. Chem. Soc.* **2006**, *128*, 6026.
(29) Wang, S.; Liang, Z.; Liu, T.; Wang, B.; Zhang, C. *Nanotechnology* **2006**, *17*, 1551.
(30) Valentini, L.; Macan, J.; Armentano, I.; Mengoni, F.; Kenny, J. M. *Carbon* **2006**, *44*, 2196.
(31) Li, H.; Cheng, F.; Duft, A. M.; Adronov, A. *J. Am. Chem. Soc.* **2005**, *127*, 14518.
(32) Sawada, H.; Shindo, K.; Ueno, K.; Hamazaki, K. *Polym. Adv. Technol.* **2005**, *16*, 764.
(33) Nakamura, T.; Ishihara, M.; Ohana, T.; Tanaka, A.; Koga, Y. *Chem. Commun.* **2004**, 1336.
(34) Dyke, C. A.; Tour, J. M. *J. Phys. Chem. A* **2004**, *108*, 11151.
(35) Peng, H.; Alemay, L. B.; Margrave, J. L.; Khabashesku, V. N. *J. Am. Chem. Soc.* **2003**, *125*, 15174.
(36) Long, L.; Lu, X.; Tian, F.; Zhang, Q. *J. Org. Chem.* **2003**, *68*, 4495.
(37) Tian, W. Q.; Liu, L. V.; Wang, Y. A. *Phys. Chem. Chem. Phys.* **2006**, *8*, 3528.
(38) Yeung, C. S.; Liu, L. V.; Wang, Y. A. *J. Theor. Comput. Nanosci.* **2007**, *4*, 1108.
(39) Boul, P. J.; Liu, J.; Mickelson, E. T.; Huffman, C. B.; Ericson, L. M.; Chiang, I. W.; Smith, K. A.; Colbert, D. T.; Hauge, R. H.; Margrave, J. L.; Smalley, R. E. *Chem. Phys. Lett.* **1999**, *310*, 367.
(40) Mickelson, E. T.; Chiang, I. W.; Zimmermann, J. L.; Boul, P. J.; Lozano, J.; Liu, J.; Smalley, R. E.; Hauge, R. H.; Margrave, J. L. *J. Phys. Chem. B* **1999**, *103*, 4318.
(41) Holzinger, M.; Vostrowsky, O.; Hirsch, A.; Hennrich, F.; Kappes, M.; Weiss, R.; Jellen, F. *Angew. Chem., Int. Ed.* **2002**, *40*, 4002.

(42) Georgakilas, V.; Kordatos, K.; Prato, M.; Guldi, D. M.; Holzinger, M.; Hirsch, A. *J. Am. Chem. Soc.* **2002**, *124*, 760.
(43) Tagmatarchis, N.; Georgakilas, V.; Prato, M.; Shinohara, H. *Chem. Commun.* **2002**, 2010.
(44) Sung, S. L.; Tsai, S. H.; Tseng, C. H.; Chiang, F. K.; Liu, X. W.; Shih, H. C. *Appl. Phys. Lett.* **1999**, *74*, 197.
(45) Gai, P. L.; Stephan, O.; McGuire, K.; Rao, A. M.; Dresselhaus, M. S.; Dresselhaus, G.; Colliex, C. *J. Mater. Chem.* **2004**, *14*, 669.
(46) Branz, W.; Billas, I. M. L.; Malinowski, N.; Tast, F.; Heinebrodt, M.; Martin, T. P. *J. Chem. Phys.* **1998**, *109*, 3425.
(47) Poblet, J. M.; Munoz, J.; Winkler, K.; Cancilla, M.; Hayashi, A.; Lebrilla, C. B.; Balch, A. L. *Chem. Commun.* **1999**, *6*, 493.
(48) Kong, Q.; Zhuang, J.; Li, X.; Cai, R.; Zhao, L.; Qian, S.; Li, Y. *Appl. Phys. A* **2002**, *75*, 367.
(49) Lu, G.; Deng, K.; Wu, H.; Yang, J.; Wang, X. *J. Chem. Phys.* **2006**, *124*, 054305.
(50) Changgeng, D.; Jinlong, Y.; Xiangyuan, C.; Chan, C. T. *J. Chem. Phys.* **1999**, *111*, 8481.
(51) Peng, S.; Cho, K. *Nano Lett.* **2003**, *3*, 513.
(52) Bekyarova, E.; Davis, M.; Burch, T.; Itkis, M. E.; Zhao, B.; Sunshine, S.; Haddon, R. C. *J. Phys. Chem. B* **2004**, *108*, 19717.
(53) da Silva, L. B.; Fagan, S. B.; Mota, R. *Nano Lett.* **2004**, *4*, 65.
(54) Lucci, M.; Reale, A.; Carlo, A. D.; Orlanducci, S.; Tamburri, E.; Terranova, M. L.; Davoli, I.; Natale, C. D.; D'Amico, A.; Paolesse, R. *Sens. Act. B* **2006**, *118*, 226.
(55) Collins, P. G.; Bradley, K.; Ishigami, M.; Zettl, A. *Science* **2000**, *287*, 1801.
(56) Kong, J.; Franklin, N. R.; Zhou, C. W.; Chapline, M. G.; Peng, S.; Cho, K. J.; Dai, H. J. *Science* **2000**, *287*, 622.
(57) Kong, J.; Chapline, M. G.; Dai, H. *Adv. Mater.* **2001**, *13*, 1384.
(58) Orita, H.; Inada, Y. *J. Phys. Chem. B* **2005**, *109*, 22469.
(59) Orita, H.; Itoh, N.; Inada, Y. *Chem. Phys. Lett.* **2004**, *384*, 271.
(60) Kačer, P.; Kuzma, M.; Červaný, L. *Appl. Catal. A* **2004**, *259*, 179.
(61) Medlin, J. W.; Allendorf, M. D. *J. Phys. Chem. B* **2003**, *107*, 217.
(62) Williams, F. J.; Palermo, A.; Tracey, S.; Tikhov, M. S.; Lambert, R. M. *J. Phys. Chem. B* **2002**, *106*, 5668.
(63) Perdew, J. P.; Burke, K.; Ernzerhof, M. *Phys. Rev. Lett.* **1996**, *77*, 3865.
(64) Hay, P. J.; Wadt, W. R. *J. Chem. Phys.* **1985**, *82*, 299.
(65) Dunning, T. H.; Hay, P. J. *Modern Theoretical Chemistry*; Plenum: New York, 1976; Vol. 3.
(66) Glendening, E. D.; Carpenter, A. E.; Weinhold, F. *NBO*, version 3.1; 1995.
(67) Reed, A. E.; Curtiss, L. A.; Weinhold, F. *Chem. Rev.* **1988**, *88*, 899.
(68) Frisch, M. J. et al. J. A. *Gaussian 03*, Revision B.05; Gaussian, Inc.: Wallingford CT, 2004.
(69) Mastrorilli, P.; Nobile, C. F.; Suranna, G. P.; Fanizzi, F. P.; Ciccarella, G.; Englert, U.; Li, Q. *Eur. J. Org. Chem.* **2004**, 1234.
(70) Puga, J.; Patrini, R.; Sanchez, K. M.; Gates, B. C. *Inorg. Chem.* **1991**, *30*, 2479.
(71) Houlis, J. F.; Roddick, D. M. *J. Am. Chem. Soc.* **1998**, *120*, 11020.
(72) Housecroft, C. E.; Sharpe, A. G. *Inorganic Chemistry*, 1st ed.; Pearson Education Limited: Essex, England, 2001.
(73) Throughout this paper, **X**Y adsorption refers to the coordination of XY to a Pt atom embedded in the side of the nanotube through the X atom.
(74) Blyholder, G. *J. Phys. Chem.* **1964**, *68*, 2772.
(75) Cotton, F. A.; Wilkinson, G.; Murillo, C. A.; Bochmann, M. *Advanced Inorganic Chemistry*, 6th ed.; John Wiley & Sons, Inc.: New York, 1999.
(76) Gajdoš, M.; Hafner, J.; Eichler, A. *J. Phys.: Cond. Matter* **2006**, *18*, 13.
(77) Weststrate, C. J.; Bakker, J. W.; Rienks, E. D. L.; Vinod, C. P.; Lizzit, S.; Petaccia, L.; Baraldi, A.; Nieuwenhuys, B. E. *Surf. Sci.* **2006**, 1991.
(78) Ranea, V. A.; Bea, E. A.; Mola, E. E.; Imbihl, R. *Surf. Sci.* **2006**, 2663.
(79) Tang, H.; Trout, B. L. *J. Phys. Chem. B* **2005**, *109*, 17630.
(80) Orita, H.; Nakamura, I.; Fujitani, T. *J. Phys. Chem. B* **2005**, *109*, 10312.
(81) Rosca, V.; Beltramo, G. L.; Koper, M. T. M. *Langmuir* **2005**, *21*, 1448.
(82) Backus, E. H. G.; Eichler, A.; Grecea, M. L.; Kleyn, A. W.; Bonn, M. *J. Chem. Phys.* **2004**, *121*, 7946.
(83) Blagojevic, V.; Flaim, E.; Jarvis, M. J. Y.; Koyanagi, G. K.; Bohme, D. K. *J. Phys. Chem. A* **2005**, *109*, 11224.
(84) Smith, G. W.; Carter, E. A. *J. Phys. Chem.* **1991**, *95*, 2327.
(85) Natile, G.; Intini, F. P.; Bertani, R.; Michelin, R. A.; Mozzon, M.; Sbovata, S. M.; Venzo, A.; Seraglia, R. *J. Organomet. Chem.* **2005**, *690*, 2121.
(86) Miao, R.; Yang, G.; Miao, Y.; Mei, Y.; Hong, J.; Zhao, C.; Zhu, L. *Rapid Comm. Mass Spec.* **2005**, *19*, 1031.
(87) Bernhardt, G.; Brunner, H.; Gruber, N.; Lottner, C.; Pushpan, S. K.; Tsuno, T.; Zabel, M. *Inorg. Chim. Acta* **2004**, *357*, 4452.
(88) Baik, M.-H.; Friesner, R. A.; Lippard, S. J. *Inorg. Chem.* **2003**, *42*, 8615.
(89) Belyaev, A. N.; Panina, N. S.; Simanova, S. A. *Russ. J. Gen. Chem.* **2003**, *73*, 1665.
(90) Lau, J. K.-C.; Deubel, D. V. *Chem. Eur. J.* **2005**, *11*, 2849.
(91) Novell-Leruth, G.; Valcárcel, A.; Clotet, A.; Ricart, J. M.; Pérez-Ramírez, J. *J. Phys. Chem. B* **2005**, *109*, 18061.
(92) Vidal-Iglesias, F. J.; Solla-Gullón, J.; Pérez, J. M.; Aldaz, A. *Electrochem. Commun.* **2006**, *8*, 102.
(93) Ford, D. C.; Xu, Y.; Mavrikakis, M. *Surf. Sci.* **2005**, *587*, 159.
(94) Wallin, M.; Grönbeck, H.; Spetz, A. L.; Skoglundh, M. *Appl. Surf. Sci.* **2004**, *235*, 487.
(95) Murray, B. J.; Walter, E. C.; Penner, R. M. *Nano Lett.* **2004**, *4*, 665.
(96) Sobczyk, D. P.; de Jong, A. M.; Hensen, E. J. M.; van Santen, R. A. *J. Catal.* **2003**, *219*, 156.
(97) Burgess, B. K.; Lowe, D. J. *Chem. Rev.* **1996**, *96*, 2983.
(98) Behder, D. *Coord. Chem. Rev.* **1999**, *182*, 297.
(99) MacLachlan, E. A.; Fryzuk, M. D. *Organometallics* **2006**, *25*, 1530.
(100) Allen, A. D.; Senoff, C. V. *J. Chem. Soc., Chem. Commun.* **1965**, 621.
(101) Kilgore, U. J.; Yang, X.; Tomaszewski, J.; Huffman, J. C.; Mindiola, D. J. *Inorg. Chem.* **2006**, *45*, 10712.
(102) McMurry, J., *Organic Chemistry*, 6th ed.; Brooks/Cole−Thomson Learning: Belmont, CA, 2004.
(103) Knowles, W. S.; Sabacky, M. J.; Vineyard, B. D. *J. Chem. Soc., Chem. Commun.* **1972**, 10.
(104) Kagan, H. B.; Dang, T. P. *J. Am. Chem. Soc.* **1972**, *94*, 6429.
(105) Dillon, A. C.; Jones, K. M.; Bekkedahl, T. A.; Kiang, C. H.; Bethune, D. S.; Heben, M. J. *Nature* **1997**, *386*, 377.
(106) Öfner, H.; Zaera, F. *J. Phys. Chem.* **1997**, *101*, 396.
(107) Stuve, E. M.; Madix, R. J. *J. Phys. Chem.* **1985**, *89*, 3183.
(108) Avery, N. R. *Langmuir* **1988**, *4*, 445.
(109) Stair, P. C.; Somorjai, G. A. *J. Chem. Phys.* **1977**, *66*, 2036.